

## In–out asymmetry of low-Z impurity deposition on the JT-60U divertor tiles

K. Masaki <sup>a,\*</sup>, J. Yagyū <sup>a</sup>, Y. Miyo <sup>a</sup>, Y. Gotoh <sup>a</sup>, T. Arai <sup>a</sup>, T. Hayashi <sup>a</sup>,  
K. Kodama <sup>a</sup>, T. Sasajima <sup>a</sup>, A. Kaminaga <sup>a</sup>, T. Tanabe <sup>b</sup>, N. Miya <sup>a</sup>

<sup>a</sup> JT-60 Facilities Division II, Department of Fusion Facilities, Naka Fusion Research Establishment,

Japan Atomic Energy Research Institute, 801 Mukouyama, Naka-machi, Naka-gun, Ibaraki-ken 311-0193, Japan

<sup>b</sup> Nagoya University, Center for Integrated Research in Science and Engineering, Furo-cho, Chikusa-ku, Nagoya 464-8603, Japan

### Abstract

Low-Z impurity (<sup>7</sup>Be) on the JT-60U divertor tiles was analyzed to study the impurity behavior in the divertor region. The amount of the <sup>7</sup>Be increased approximately one hundred times after B<sub>4</sub>C-tile installation in the outer divertor. The <sup>7</sup>Be was probably produced by <sup>10</sup>B(p,α)<sup>7</sup>Be nuclear reaction on the divertor tiles in the hydrogen experiment with ion cyclotron range of frequency heating. The <sup>7</sup>Be was distributed asymmetrically in the poloidal and the toroidal direction. The highest <sup>7</sup>Be concentration was found at the inner divertor whose boron content (B/(B+C) ~ 20%) was lower than the B<sub>4</sub>C tiles (B/(B+C) ~ 80%) of the outer divertor. This result may imply impurity transport from the outer divertor to the inner divertor.

© 2004 Elsevier B.V. All rights reserved.

### 1. Introduction

For future fusion devices, studies of erosion/re-deposition and impurity transport are very important to understand the plasma surface interactions. In particular, interactions between plasma and carbon-based materials have been intensively studied so far. A remarkable erosion/deposition asymmetry between the inner and outer divertor targets was observed in many tokamaks [1,2]. Also in JT-60U, the erosion/deposition asymmetry was observed. The inner divertor was a redeposition-dominated region, whereas the outer divertor was an erosion-dominated region [3]. However, the carbon impurity behavior in the divertor region is not fully understood yet.

In JT-60U, carbon fiber composite (CFC) and isotropic graphite are used as armor tiles on most plasma facing components. Various radioactivity elements

(tritium, beryllium (<sup>7</sup>Be), cobalt (<sup>60</sup>Co), etc.) were detected in radioactivity analyses of the armor tiles. With respect to the tritium in the plasma facing wall, the distribution and the retention processes were already reported [4]. The cobalt is believed to originate from the vacuum vessel and in-vessel component materials (Inconel 625 and SUS316). In JT-60U, radioactive beryllium (<sup>7</sup>Be) was found on all plasma facing tiles. In particular, installation of the B<sub>4</sub>C tiles, which were selected in order to reduce chemical sputtering of CFC tiles as well as oxygen impurity [5,6], increased the amount of <sup>7</sup>Be approximately one hundred times. The <sup>7</sup>Be was probably produced by the <sup>10</sup>B(p,α)<sup>7</sup>Be reaction. Furthermore, the <sup>7</sup>Be was distributed asymmetrically in the poloidal and toroidal direction. This <sup>7</sup>Be distribution may give useful information on impurity behavior. For the study of the impurity behavior, i.e. in–out asymmetry of the impurity deposition on the divertor targets, we focused on the radioactive beryllium.

In this paper, results of <sup>7</sup>Be analyses of the divertor tiles are described. In addition, mechanism of <sup>7</sup>Be production and impurity transport in the divertor region are discussed.

\* Corresponding author. Tel.: +81-29 270 7432; fax: +81-29 270 7449.

E-mail address: [masakik@fusion.naka.jaeri.go.jp](mailto:masakik@fusion.naka.jaeri.go.jp) (K. Masaki).

## 2. Sample tiles

Samples for the analyses of beryllium ( $^7\text{Be}$ ) were the divertor tiles removed from the open divertor (1991–1997) and the W-shaped divertor (1997 onwards). In JT-60U, boronization using decaborane as one of the wall conditioning techniques to reduce oxygen impurity has been performed since 1992 [7–9]. The open divertor had eight rows (a, b–h) of tiles in the poloidal direction. In December 1992, CFC tiles with a  $\text{B}_4\text{C}$ -converted layer (i.e.  $\text{B}_4\text{C}$  tiles) of  $\sim 100\ \mu\text{m}$  thickness were installed in the outer divertor row-f [5]. CFC tiles having a  $\text{B}_4\text{C}$ -converted layer of  $\sim 300\ \mu\text{m}$  thickness were installed in the outer divertor row-e in December 1993 [6]. The sample tiles of the open divertor were removed in November 1992, 1993 and 1994. Accordingly, the 1992-year samples experienced only the boronization. The thickness of the boron layer formed by the boronization was  $\sim 100\ \text{nm}$  [7]. The samples removed in 1993 and 1994 experienced  $\text{B}_4\text{C}$ -tile operation and boronization. The sample tiles of the W-shaped divertor, which has no  $\text{B}_4\text{C}$  tiles, were removed in November 1998. These samples experienced boronization forming a boron layer of  $\sim$ several  $100\ \text{nm}$  [9].

Table 1 shows experimental conditions in each year. The heating parameters of ion cyclotron range of frequency (ICRF) are those in hydrogen experiments performed in the last phase of each year-long experimental campaign. In 1993 and 1994, hydrogen experiments with relatively high ICRF heating power of 3–5 MW and integrated injection times of 100–200 s were performed. In 1998, the ICRF power and integrated injection time

Table 1  
Experimental conditions in each year

Operation year	1992	1993	1994	1998
Average ICRF power (MW)	2.1	4.7	2.5	2.9
Integrated ICRF injection time (s)	86	218	103	55
Number of ICRF shot (shots)	53	162	98	46
Number of boronization	1	2	1	1
$\text{B}_4\text{C}$ -tile operation		Row-f $\sim 100\ \mu\text{m}$	Row-f $\sim 100\ \mu\text{m}$ , row-e $\sim 300\ \mu\text{m}$	

The ICRF heating parameters are those in hydrogen experiments performed in the last phase of each year-long experimental campaign. After the  $\text{B}_4\text{C}$  tile ( $300\ \mu\text{m}$ ) installation in December 1993, boron impurity in plasma was increased.

in the hydrogen experiments were  $\sim 3\ \text{MW}$  and  $\sim 50\ \text{s}$ , respectively.

The  $^7\text{Be}$  content of each tile was measured without cutting samples, using a germanium semiconductor detector and a NaI scintillation detector.

## 3. $^7\text{Be}$ distribution in open divertor and W-shaped divertor

Fig. 1 shows beryllium ( $^7\text{Be}$ ) poloidal distribution of the open divertor tiles removed in November 1992, 1993 and 1994. These data were estimated values for end of each year-experimental campaign, because of the relatively short half-life (53.3 d). After the installation of  $\text{B}_4\text{C}$  tiles, the  $^7\text{Be}$  concentrations of the divertor tiles increased from  $\sim 10$  to  $\sim 10^3\ \text{Bq/cm}^2$ . In particular, the samples removed in 1994, which experienced thick  $\text{B}_4\text{C}$  tile ( $\sim 300\ \mu\text{m}$ ) operation, had a high  $^7\text{Be}$  level. The highest  $^7\text{Be}$  concentration of  $16\ \text{kBq/cm}^2$  was found at row-c of the inner divertor. The  $^7\text{Be}$  concentration at the inner divertor was always higher than that at the outer divertor. Moreover,  $^7\text{Be}$  levels of row-e increased after  $\text{B}_4\text{C}$ -tile installation in row-e. Full toroidal measurement of row-e tiles showed that the  $^7\text{Be}$  was distributed peri-

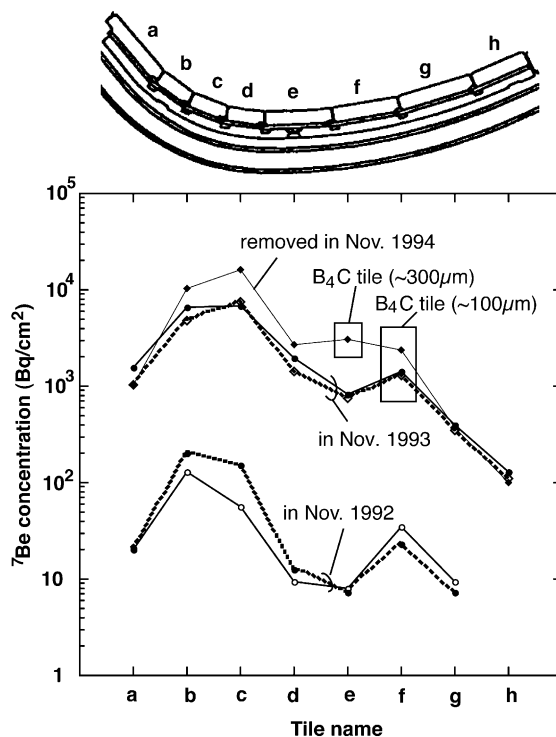


Fig. 1. Beryllium ( $^7\text{Be}$ ) poloidal distribution in the open divertor tiles removed in November 1992, 1993 and 1994. The dot lines are sample tiles removed from different toroidal positions. The  $^7\text{Be}$  was measured using a germanium semiconductor detector.

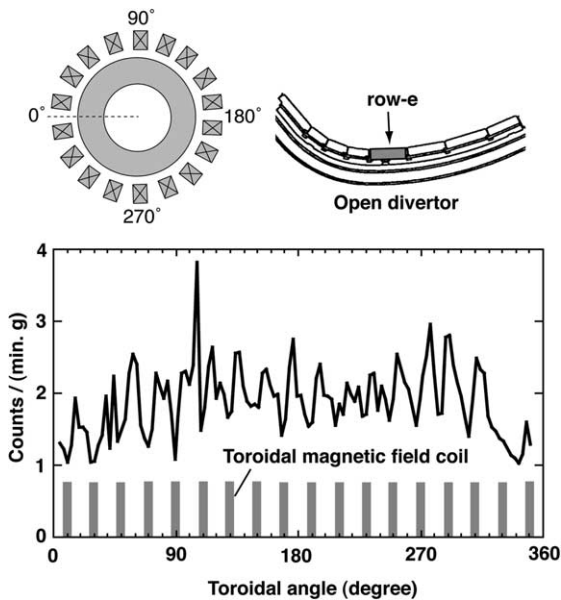


Fig. 2.  $^7\text{Be}$  toroidal distribution in the divertor tiles (row-e) removed in November 1993. Since the dominant radioactive impurity in the divertor tiles was  $^7\text{Be}$ , full toroidal measurement of row-e was performed using a NaI scintillation detector without nuclide identification.

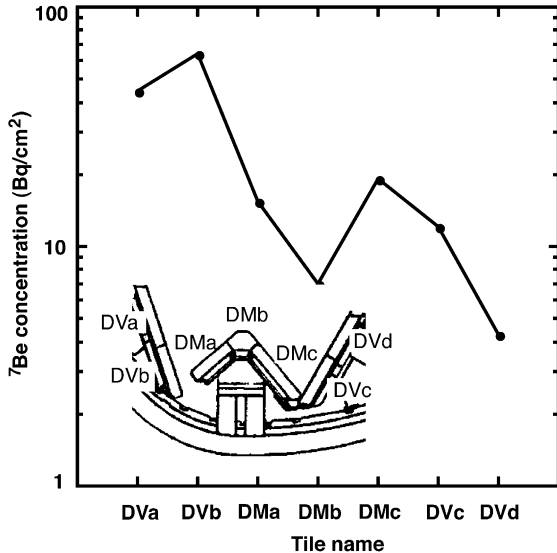


Fig. 3.  $^7\text{Be}$  poloidal distribution in the W-shaped divertor tiles removed in 1998. The  $^7\text{Be}$  was measured using a germanium semiconductor detector.

odically in the toroidal direction as shown in Fig. 2. This distribution was correlated to the toroidal field coil (TFC) positions. Fig. 3 shows  $^7\text{Be}$  poloidal distribution in the W-shaped divertor tiles removed in November

1998. The  $^7\text{Be}$  concentration decreased to  $\sim 10$  Bq/cm $^2$  after the divertor modification. Also in the W-shaped divertor, the  $^7\text{Be}$  concentration at the inner divertor was higher than that at the outer divertor.

## 4. Discussion

### 4.1. Production of $^7\text{Be}$

After the  $\text{B}_4\text{C}$  installation, the  $^7\text{Be}$  concentration increased drastically approximately one hundred times. In the W-shaped divertor without  $\text{B}_4\text{C}$  tiles,  $^7\text{Be}$  decreased to the level before the installation of the  $\text{B}_4\text{C}$  tiles. This result must indicate that  $^7\text{Be}$  in JT-60U originated from boron. Most probably,  $^7\text{Be}$  was produced by the  $^{10}\text{B}(p,\alpha)^7\text{Be}$  reaction. The cross section at the resonance peak (1.5 MeV) is 0.21 barn. In JT-60U, high energy protons are produced by D–D nuclear reactions and in a hydrogen plasma with ICRF heating performed in the last phase of a year-long experimental campaign. The energy of the proton produced by D–D nuclear reaction is 3 MeV. The integrated amount of the proton production was  $\sim 1 \times 10^{19}$  in each year (average  $\sim 3 \times 10^{15}$ /shot). According to the simulation using an orbit following Monte Carlo code [10], roughly 30% of the produced protons were implanted into the divertor tiles (rows a–h) with average energy of  $\sim 1.5$  MeV. Taking account of the proton production in the deuterium experiments and the  $^7\text{Be}$  production yield [11] and the half-life of  $^7\text{Be}$  (53.3 d), the total amount of the  $^7\text{Be}$  at the divertor region was estimated to be  $\sim 10^6$  Bq even assuming that a thick boron layer of 30  $\mu\text{m}$  exists on the divertor tiles, which is equal to the penetration depth of 1.5 MeV protons. This amount of  $^7\text{Be}$  was very low compared with that of the samples removed in 1993 and 1994 ( $\sim 10^8$  Bq). In the hydrogen experiment with ICRF heating, the hydrogen ions are accelerated to several MeV [12]. The number of high energy protons produced by ICRF heating is expected to be larger ( $\sim 10^{16} \text{ m}^{-3}$  [13]) than the number of protons produced by D–D nuclear reaction. This suggests that most of  $^7\text{Be}$  was probably produced by the  $^{10}\text{B}(p,\alpha)^7\text{Be}$  reaction in the hydrogen experiments with ICRF heating and  $\text{B}_4\text{C}$  tiles.

Furthermore, the following two cases should be considered for the  $^7\text{Be}$  production. (1) Boron on the tile surface was bombarded by high energy protons due to ripple losses. (2) Boron reacted with high energy proton in the plasma. The periodic  $^7\text{Be}$  distribution in the toroidal direction, which was correlated to TFC positions (i.e. ripple loss), and increase of  $^7\text{Be}$  at row-e after  $\text{B}_4\text{C}$ -tile installation (row-e) in 1993 probably reflected the high energy proton bombardment of the tile surface.

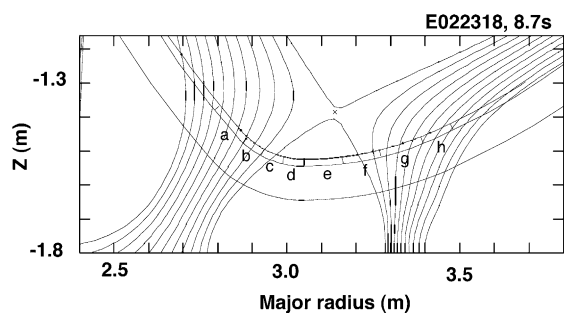


Fig. 4. Typical divertor configuration in 1994 hydrogen experiments. The ICRF heating power and plasma current were 2.5 MW and 2.5 MA, respectively. The inner and the outer strike points were located at row-c and row-f, respectively.

#### 4.2. Transport of $^7\text{Be}$

With respect to the poloidal distribution,  $^7\text{Be}$  in the inner divertor was always higher than that in the outer divertor. Fig. 4 shows a typical divertor configuration in 1994 hydrogen experiments. In this case, it is expected that the high energy protons impinged on the tiles of the private region and the outer divertor region, because the ripple rate of the toroidal magnetic field was high on the low field side. However, the highest  $^7\text{Be}$  concentration was found at row-c, whose boron content ( $\text{B}/(\text{B}+\text{C}) \sim 20\%$ ; X-ray photoelectron spectroscopy analysis) was lower than  $\text{B}_4\text{C}$  tiles. In the scanning electron microscope analyses of the divertor tiles removed in November 1994, a thick deposition layer of  $\sim 60 \mu\text{m}$  was found on the inner divertor tile (row-b), whereas no continuous deposition layer was observed on the outer divertor tiles. Also in the W-shaped divertor, it was reported that the inner divertor was a deposition-dominated region, whereas the outer divertor was an erosion-dominated region [3]. These results may imply impurity transport from the outer divertor to the inner divertor.

#### 5. Conclusions

In JT-60U, various radioactive elements (tritium, beryllium ( $^7\text{Be}$ ), cobalt ( $^{60}\text{Co}$ ), etc.) were detected in radioactivity analyses of the armor tiles. For the study of the impurity behavior in the divertor region,  $^7\text{Be}$  on the divertor tiles was analyzed. Furthermore, in–out asym-

metry of the  $^7\text{Be}$  and the impurity transport in the divertor region were discussed.

Beryllium ( $^7\text{Be}$ ) produced by the  $^{10}\text{B}(\text{p},\alpha)^7\text{Be}$  nuclear reaction in the hydrogen experiment with ion cyclotron range of frequency heating was distributed asymmetrically in the poloidal and toroidal directions. The  $^7\text{Be}$  was periodically distributed in the toroidal direction, which was correlated to toroidal field coil positions, i.e. ripple loss. Therefore,  $^7\text{Be}$  was believed to be produced by proton bombardment of the tile surface. With respect to the poloidal direction, the  $^7\text{Be}$  concentration in the inner divertor was higher than that in the outer divertor ( $\text{B}_4\text{C}$ ). This result may imply impurity transport from the outer divertor to the inner divertor.

#### Acknowledgements

The authors would like to thank the JT-60 team for their contributions to the operation and the experiments of JT-60U.

#### References

- [1] D.G. Whyte, J.P. Coad, P. Franzen, et al., Nucl. Fusion 39 (1999) 1025.
- [2] G. Federici, C.H. Skinner, J.N. Brooks, et al., Nucl. Fusion 41 (2001) 1967.
- [3] Y. Gotoh, J. Yagyu, K. Masaki, et al., J. Nucl. Mater. 313–316 (2003) 370.
- [4] K. Masaki, K. Sugiyama, T. Tanabe, et al., J. Nucl. Mater. 313–316 (2003) 514.
- [5] T. Ando, K. Kodama, M. Matsukawa, et al., in: Proceedings of the 15th Symposium on Fusion Engineering, 1993.
- [6] T. Ando, K. Masaki, K. Kodama, et al., J. Nucl. Mater. 220–222 (1995) 380.
- [7] M. Saidoh, N. Ogiwara, M. Shimada, et al., Jpn. J. Appl. Phys. 32 (1993) 3276.
- [8] J. Yagyu, N. Ogiwara, M. Saidoh, et al., J. Nucl. Mater. 214–243 (1997) 579.
- [9] J. Yagyu, T. Arai, A. Kaminaga, et al., in: Proceedings of the 15th Symposium on Fusion Engineering, 2002.
- [10] K. Tani, M. Azumi, H. Kishimoto, et al., J. Phys. Soc. Jpn. 50 (1981) 1726.
- [11] R.J. Peterson, C.S. Zaidins, M.J. Fritts, et al., Ann. Nucl. Energy 2 (1975) 503.
- [12] H. Kimura, M. Saigusa, T. Kondoh, et al., J. Plasma Fusion Res. 71 (1995) 1147.
- [13] T. Kondoh, H. Kimura, Y. Kusama, et al., J. Plasma Fusion Res. 72 (1996) 1397.